Research Article | Vol. 10, No. 12 / 1 December 2019 / Biomedical Optics Express 6422
Biomedical Optics EXPRESS

Optical detection of the structural properties of tumor tissue generated by xenografting of drug-sensitive and drug-resistant cancer cells using partial wave spectroscopy (PWS)

PRAKASH ADHIKARI,[1] PRASHANTH K. B. NAGESH,[2] FATEMAH ALHARTHI,[1] SUBHASH C. CHAUHAN,[2] MEENA JAGGI,[2] MURALI M. YALLAPU,[2,4] AND PRABHAKAR PRADHAN[1,3]

[1]*Department of Physics and Astronomy, Mississippi State University, Mississippi State, MS 39762, USA*
[2]*Department of Immunology and Microbiology, School of Medicine, University of Texas-Rio Grande Valley, McAllen, TX 78504, USA*
[3]*pp838@msstate.edu*
[4]*murali.yallapu@utrgv.edu*

Abstract: A mesoscopic physics-based optical imaging technique, partial wave spectroscopy (PWS), has been used for the detection of cancer by probing nanoscale structural alterations in cells/tissue. The development of drug-resistant cancer cells/tissues during chemotherapy is a major challenge in cancer treatment. In this paper, using a mouse model and PWS, the structural properties of tumor tissue grown in 3D structures by xenografting drug-resistant and drug-sensitive human prostate cancer cells having 2D structures, are studied. The results show that the 3D xenografted tissues maintain a similar hierarchy of the degree of structural disorder properties as that of the 2D original drug-sensitive and drug-resistant cells.

1. Introduction

Elastic light scattering, especially in the visible range of light, is an important method for probing structural morphologies of the biological cells/tissues. It is now shown that probing the structural alterations at nano to submicron scale enables the prediction of several properties of the physical condition of cells/tissues in normal and disease/abnormal states. Recent studies have shown that the progression of carcinogenesis results in nanoscale structural alterations due to the rearrangement of the basic building blocks, in particular, macromolecular components inside the cells/tissues. This nanoscale structural alterations, in terms of the degree of disorder strength, has been shown as an important biomarker in the determination of cancer stages [1,2]. However, the histopathological examinations of cells/tissues, conventionally, are based on a large degree of changes in the cellular architecture, mainly nuclear size, during the disease process [3–6]. Also, the sensitivity of the existing pathological optical microscopic techniques used to detect such nanoscale alterations are restricted by the diffraction limited resolution (>∼200 nm).

A recently introduced spectroscopic microscopy technique, partial wave spectroscopy (PWS), which combines the interdisciplinary approaches of mesoscopic condensed matter physics and microscopic imaging, to quantify the degree of change of the nanoscale structural disorder of weakly disorder medium like biological cells/tissues [7–11]. The statistical quantifications of the reflected intensities due to the nanoscale refractive index fluctuations of the biological cells/tissues are carried out using the PWS analysis. In the PWS technique, the backscattering signals from thin weakly disordered cell/tissue samples are divided into many parallel scattering quasi one-dimensional reflections to calculate the structural disorder strength of the samples. Further, the spatial variation of the intracellular components such as DNA, RNA, lipids, and

#381657 https://doi.org/10.1364/BOE.10.006422
Journal © 2019 Received 25 Oct 2019; accepted 6 Nov 2019; published 21 Nov 2019

Biomedical Optics EXPRESS

extracellular matrices (ECM) gives rise to spatial mass density fluctuations in terms of the refractive index fluctuations of the cells/tissues. This spatial refractive index fluctuations can be quantified in terms of the degree of structural disorder. The degree of structural disorder parameter L_d, called the disorder strength, can quantify nanoscale alterations and distinguish different cancer stages with higher accuracy. For a quasi-1D approximation, the disorder strength can be expressed as $L_d = dn^2 \times l_c$, where dn is the standard deviation (std) of the onsite refractive index fluctuations $dn(r)$ and l_c is its spatial correlation length. The efficiency and application of the PWS technique in measuring nanoscale alterations, i.e. the L_d parameter, to diagnose diseases like cancer has been developed and explored [7–10,12,13]. The detection of molecular specific structural disorder in submicron scales of control and cancer/abnormal cell nuclei are also studied by the light localization technique using confocal microscopy, which support the increase in the molecular specific structural disorder in progressive cancer [14–17].

After diagnosis of cancer, the cancer patient generally goes through chemotherapy drug treatment. Resistant of cancer cells/tissues to chemotherapy drug is one of the obstacles to cancer treatment. Recently, the PWS technique was successfully used to study the effect of chemotherapy drugs on prostate cancer cell lines and to quantitatively measure the structural disorder strength of drug-sensitive and drug-resistant prostate cancerous cells [8]. The results show that the chemo-resistant cells have a higher degree of structural disorder than that of the chemo-sensitive cells. Drug-resistant cancerous cells can survive through chemotherapy drug treatment, as the different mechanisms and morphological structures developed are responsible for drug resistance. These different morphological structures in drug-resistant cancer cells may be due to the rearrangements of macromolecules, increase in the sizes of pores, architectural differences of the cytoskeletal network, etc., which result in increasing aggressiveness and the disorder strength.

Prostate cancer is one of the most prevalent types of cancer with one of the highest male mortality rates in the USA. The American Cancer Society (ACS) estimates about 174,650 new cases of prostate cancer will appear and account for a total of 31,620 deaths for 2019. Across the globe, the statistical data of prostate cancer suggests that among every 9 men, one individual will develop this cancer during his lifespan. Therefore, it is necessary to explore early and effective diagnosis and treatment methods for prostate cancer. At present, chemotherapy is the only way to treat metastasized prostate cancer, however, it is often found ineffective due to an individual patient's chemo-resistance that leads to tumor progression [8,18–22]. The PWS studies of cancer cell lines have shown some promising success in distinguishing the hierarchy and drug effectiveness based on the measurement of the biomarker, the structural disorder strength L_d [8].

These PWS studies of drug resistance cells were mainly focused on isolated cancer cells which were grown in 2D on glass slides. However, in reality, a metastasized cancer cell grows into a tumor with 3D structure when grown within the body, and these tumor cells may have different structural properties due to its grown 3D tissue structures. This leads to a demand for the development and quantitative characterization of 3D tumor tissues that are grown from the drug-sensitive and drug-resistant cancer cells. This could establish a correlation between isolated cells of 2D structure which is grown into tissue in 3D structure, based on the structural disorder. In particular, we want to verify the structural properties of 3D tissues generated by xenografting of cancer cells, and to understand any relationship between the 3D tissue structures with their original 2D cell structures, using the L_d parameter. Human cancer cases have been studied by innumerable murine methods and the determinants responsible for malignant transformation, invasion, and metastasis, as well as the examination of the response to therapy is investigated by the aid of these murine models. Xenografting of human cancer cells in a mouse model is one of the most extensively used models to study the development of tumors from cells [23,24]. Cancerous human cells were subcutaneously injected in immunocompromised mice. Based on the number of cells injected, the tumors will develop over 1-8 weeks and reaction to the proper

Biomedical Optics EXPRESS

therapeutic regimes can be studied *in vivo* [23,25] or *ex vivo*. At the same time, the structural properties of growing xenografted cancer cells are not well studied.

In this work, using a further engineered PWS technique, we explore the structural properties of the 3D tumor tissues obtained by xenografting drug-sensitive and drug-resistant human prostate cancer cells (2D structures) using a mouse model. We study structural properties of tissues obtained by xenografting two types of human prostate cancer (PC) cell lines, namely DU145 and PC3, whose drug-resistant and drug-sensitive structural properties were studied earlier by the PWS technique [8]. From the results, a correlation between the 3D structural disorder of tissues original grown from chemotherapy drug-sensitive and drug-resistance cells and the original cells will be performed. Finally, we will also discuss about the potential applications of the technique in cancer diagnostics.

2. Method

2.1. PWS experimental setup

We perform the structural disorder measurement of tissues using a recently developed partial wave spectroscopy (PWS) experimental technique, with further engineering of finer focusing [7–9]. The PWS setup with a fine focus to measure the structural alterations at the nanoscale level is as shown in Fig. 1. Xenon Lamp (Newport, 150W), a source of stable broadband white light is used to illuminate tissue samples of micron thickness using Kohler Illumination. The white light is reflected towards the combination of lenses with silver coated mirror (Thorlabs, f = 50.8mm). The combination of converging lenses (Thorlabs, f = 50.8 mm) along with the apertures (Newport) form a 4f system that helps to minimize the diffraction effect and preserve the high-frequency effect and hence enhances the sharpness in an image. This collimated light from the lens is reflected by a right-angle prism (Thorlabs, 25.4 mm) and passed through the dichroic mirror (Thorlabs, 25.4 mm) and then enters an objective lens (Newport, NA = 0.65,40X). The low numerical aperture objective lens focuses the light in the sample within its working distance with the help of high-resolution 3D electronic motorized stage (Zebar Tech, 100 nm in Z axis and 40 nm in X-Y axis). This high-resolution motorized 3D stage is considered revolutionary to the microscopic setup for its extreme accuracy and finer focus. A finer focus is essential for correctly defining the effective scattering volume/length of a sample. The backscattered signal from the sample is passed through the objective which gets reflected into the thick collecting lens (Thorlabs, Φ=50.8 mm) before the aperture. Finally, the collected backscattered signal passes through a liquid crystal tunable filter i.e. LCTF (Thorlabs, KURIOS-WB1) with a spectral resolution of 1 nm within the visible range (420-730 nm) of the spectrum. A CCD camera (Retiga 3, 1460×1920) coupled with a LCTF controller records the filtered signal in the desired wavelength range. Here, the CCD camera and LCTF filter are coupled with the LCTF controller in such a way that for each 1 nm increment in wavelength by the LCTF filter (resolution 1 nm), the backscattered signals are recorded in the CCD within the visible range.

2.2. Calculation of the structural disorder or disorder strength (L_d)

The backscattered images are recorded in the CCD camera at every wavelength (λ) at the spatial pixel position (x, y) in the wavelength range 450-700 nm, and the reflected data cube, $R(x, y; \lambda)$, is acquired by the PWS system. Here, the data cube $R(x, y;\lambda)$ includes the fluctuating part of the reflection coefficient over the visible wavelength regime due to the presence of a disordered medium including the high frequency noise. In a quasi-1D approximation, the collected backscattered data at each (x, y) from $R(x, y;\lambda)$ is fitted with a polynomial of the 5^{th} order. The fitted polynomial is then extracted from the signal to remove the systematic errors. In the next step, the $R(k)$ signal for each pixel position (x, y) is obtained after applying a fifth-order low-pass Butterworth filter with a suitable normalized cutoff frequency to remove the

Biomedical Optics EXPRESS

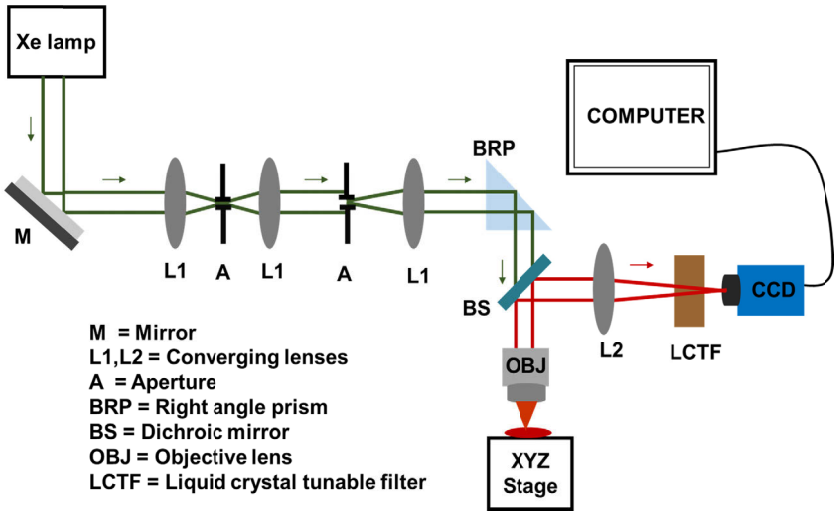

Fig. 1. Experimental layout of the partial wave spectroscopy (PWS) setup with nanoscale structural alteration sensitivity. The green color represents broadband white light from the source and red color after dichroic mirror is the backscattered signal.

high frequency noise components from the reflected signals of micron size samples. From the extracted backscattered data cube, calibration of the system is done by matching the reflected intensity pattern using a non-disordered system, NIST-traceable microspheres with the reflected signal from a thin film slab model. The PWS measures the spectral fluctuation dividing the signal from the sample into the collection of backscattered parallel channels. Based on the mesoscopic optical property of the object, the spectral fluctuations originating from multiple scatterings of the sample are analyzed.

The fluctuating part of reflection signals $R(x, y;\lambda)$ arises due to the multiple interferences of the photons reflected from the disordered medium. Since in a quasi-1D approximation, the sample is virtually divided into many parallel channels within the diffraction limited transverse size and the backscattered signals propagating along the 1D trajectories are collected. This optical detection method is termed as the partial wave spectroscopy (PWS). The statistical properties of nanoarchitecture are quantified at the nanoscale level by analyzing the fluctuating part of the reflected intensities. The refractive index fluctuation information is collected from these spectral fluctuations originated from the multiple scattering of the sample at any length scale below the diffraction limit. The degree of structural disorder parameter L_d can be derived from the *rms* value of the reflection intensity $<R(k)>_{rms}$ and the spectral auto-correlation decay of the reflection intensity $C(\Delta k)$ ratio. That means, for a given pixel at position (x, y), the degree of structural disorder is defined as [7–11]:

$$L_d = \frac{Bn_o{}^2\langle R\rangle_{rms}}{2k^2}\frac{(\Delta k)^2}{-\ln(c(\Delta k))}\Big|_{\Delta k\to 0} \tag{1}$$

Where B is the normalization constant, n_0 is the average refractive index of the biological cells/tissues, and k is the wavenumber ($k = 2\pi/\lambda$).

For the Gaussian color noise of the refractive index at position r and r' $<dn(r)dn'(r')>=dn^2exp(-|r-r'|/l_c)$, it can be shown that $L_d=<dn^2>l_c$ [10,11]. The disorder strength quantifies the variability of the local density of intracellular material within the samples, and hence the average and standard deviation of the L_d are calculated to characterize the system.

Biomedical Optics EXPRESS

2.3. Sample preparation

Freshly collected prostate cancer (PC) cells from two different cell lines were used to develop prostate xenograft mouse model. For the generation of tumor xenograft mouse models, 6–8 weeks old male nude mice were implanted with PC3 (docetaxel-sensitive and docetaxel-resistant) and DU145 (docetaxel-sensitive and docetaxel-resistant) human PC cell samples (2×10^6 cells per mice), by subcutaneously injections. After tumors reached beyond the critical size of 1000 mm^3, they were excised from euthanized mice. The excised tumors were further paraffin embedded and sectioned using microtome in 4μm thickness and placed on glass slides. Further, these slides were processed for antigen retrieval process as described previously [26]. The resultant tumor sections were subject to imaging studies.

3. Results

PWS detects the nanoscale structural alterations in the cells/tissues and can distinguish the different levels and effects of the drug in the tumorous cells/tissues [11]. Among the different types of cancer, prostate cancer is a major concern of public health at present because of its low survival rate. Further, drug-resistant cancer cells are a prominent problem currently in cancer treatment. Therefore, we focus our research to characterize the structure of tumor tissues generated by the xenografting of chemotherapy drug-sensitive and drug-resistant prostate cell lines, DU145 and PC3. For this, human drug-sensitive and drug-resistant prostate cancer cells were subcutaneously injected in mice and allowed to grow and achieve the tumor size of ~1000mm^3. After that, mice were euthanized, and tumors were excised then subsequently processed to 4 μm thick tumor sections on slides for PWS imaging analyses.

PWS experiments, as described earlier, were performed on xenografted prostate tumor tissues for each category on at least 3 different mice. All tumor tissue was obtained from different prostate cancer cell lines xenografted into mouse models. For each tissue sample, PWS experiments were performed on 7 different spots. In particular, for each category of a tumor, ~60 different spots are experimented with PWS and analyzed. The spectroscopic PWS experiments are performed in the wavelength range 450-700 nm. The backscattered data matrix $R(x, y; \lambda)$ are imported and the disorder strength for each tissue is calculated using the PWS technique as described in section 2.2. The disorder strength is calculated as the product of the variance and the spatial correlation length of the refractive index fluctuations, $L_d = \langle \Delta n^2 \rangle l_c$. The average and standard deviation of the disorder strength for each category is calculated in order to understand the physical properties of a tumor developed as a 3D structure from a cell. The detailed PWS analysis of a tumor obtained from a xenografted model of drug-sensitive and drug-resistant cell lines DU145 and PC3 are explained below:

3.1. Structural disorder in the xenografted DU145 tumor tissue type

In Fig. 2, the PWS analysis of a tumor tissues obtained from xenografting drug-sensitive and drug-resistant prostate human cancer cell lines of DU145 type are shown. From the PWS experiment $R(x, y, \lambda)$ data matrixes were obtained. At every pixel point (x, y), $R(k)_{rms}$ value and corresponding $C(\Delta k)$ were obtained, and from these two values, L_d value was calculated using Eq. (1). The bright field images, as shown in Fig. 2(a)-(b), of the thin tissue samples developed from drug-sensitive and drug-resistant cancer cell lines appear indistinguishable, whereas the L_d images, as shown in Fig. 2.(a')-(b') are noticeably distinguishable. The red spots in the L_d image represent a higher disorder strength, i.e. the L_d value of that pixel. It can be seen in the bar graphs, Fig. 2(c) and 2(d), that there is an increase in the degree of structural disorder of tumor tissue generated from xenografting drug-resistant cancer cells, compared to the tissues obtained from xenografting drug-sensitive cancer cells. The average L_d value of a tumor obtained from a drug-resistant cancer cell line is 9% higher than the tumor obtained from a drug-sensitive cancer

Biomedical Optics EXPRESS

cell line and the standard deviation *std*(L_d) is 8% higher. This result is in strong agreement with the disorder strength calculated for drug-resistant and drug-sensitive cell lines earlier [8]. The disorder strength of the prostate cancer cell line calculated using the PWS has shown that the average and standard deviation of L_d values are higher in drug-resistant cells compared to the drug-sensitive for DU145 type cells. The results confirm that the xenografted tissue structures also have similar trends to original cell structures.

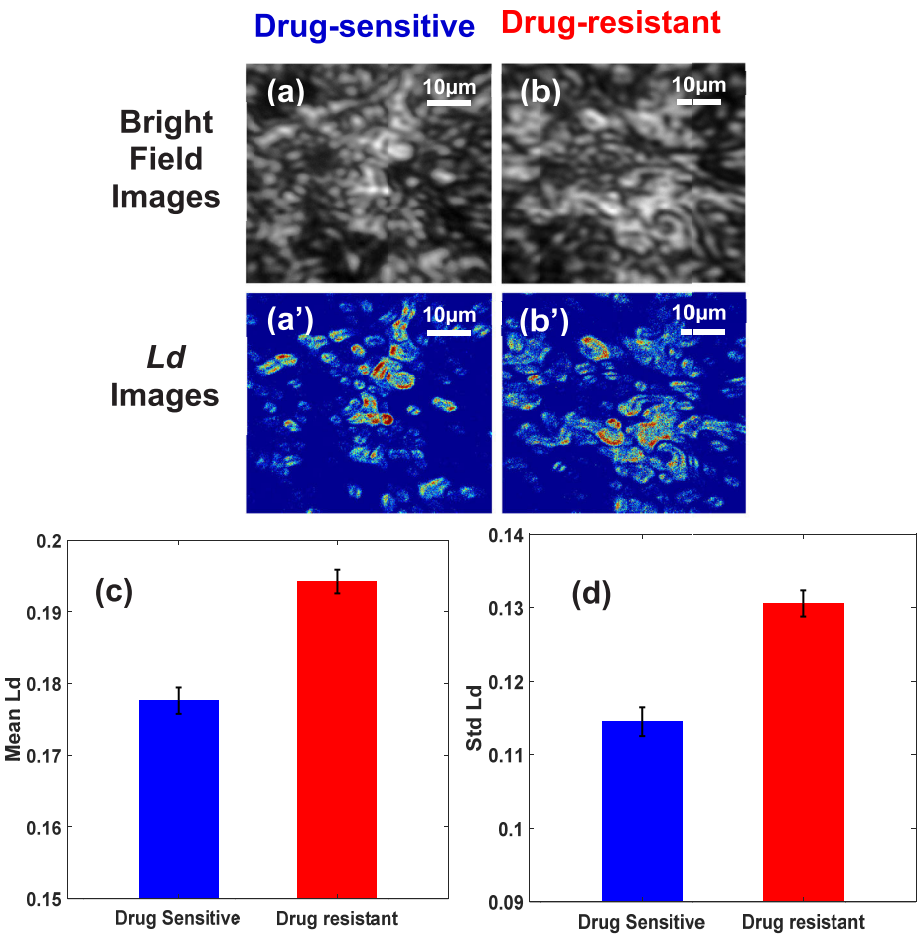

Fig. 2. (a) and (b) are the bright field images while (a') and (b') are the disorder strength, L_d images of tissue obtained by xenografting drug-sensitive and drug-resistant PC cells line of DU145 type respectively. (c) and (d) are the graphical representation of the mean and standard deviation of L_d of tumor respectively. Result shows 9% higher in the mean L_d and a 8% increase in *std* L_d in tumors developed from drug-resistant PC DU145 type cells line than the drug-sensitive cells. P-value < 0.05.

3.2. *Structural disorder in the xenografted prostate PC3 tumor tissue type*

Figure 3(a)-(b) shows the bright field and L_d images of tumor tissues originated from drug-sensitive and drug-resistant PC PC3 type cells. Based on intrinsic properties of the tissue, the disorder strength L_d at each pixel of the individual tissue image is calculated and represented by 2D color maps in Fig. 3.(a')-(b'). In the color map, red spots correspond to the higher structural disorder strength present in the thin tissue structure (averaged along the z-direction of the sample).

Biomedical Optics EXPRESS

The bar graphs, 3(c) and 3(d), are the representation of the average and standard deviation of L_d values with the standard error bars. The result shows 12% difference in the average local disorder strength L_d and 15% difference in the *std* (L_d), between tumors obtained from drug-sensitive and drug-resistant cell lines. The increment in the mean and standard deviation of L_d for tissues collected by the xenografting of drug-resistant PC PC3 cells compared to the drug-sensitive cells are consistent with the original cell structures. It is clear from the plots that the disorder strength increases from drug-sensitive to drug-resistant xenografted tumor tissues. Earlier results using PWS analysis show that PC PC3 cells are more aggressive than other cell lines and in the same way drug-resistant PC cell lines have higher disorder strength than drug-sensitive PC PC3 cells. Figures 2 and 3 show the results obtained using xenografted tissue samples also have the same kind of disorder strength hierarchy to that of the original PC cells. In particular, a comparatively higher structural disorder strength L_d for tumors obtained from drug-resistant PC3 PC cell line

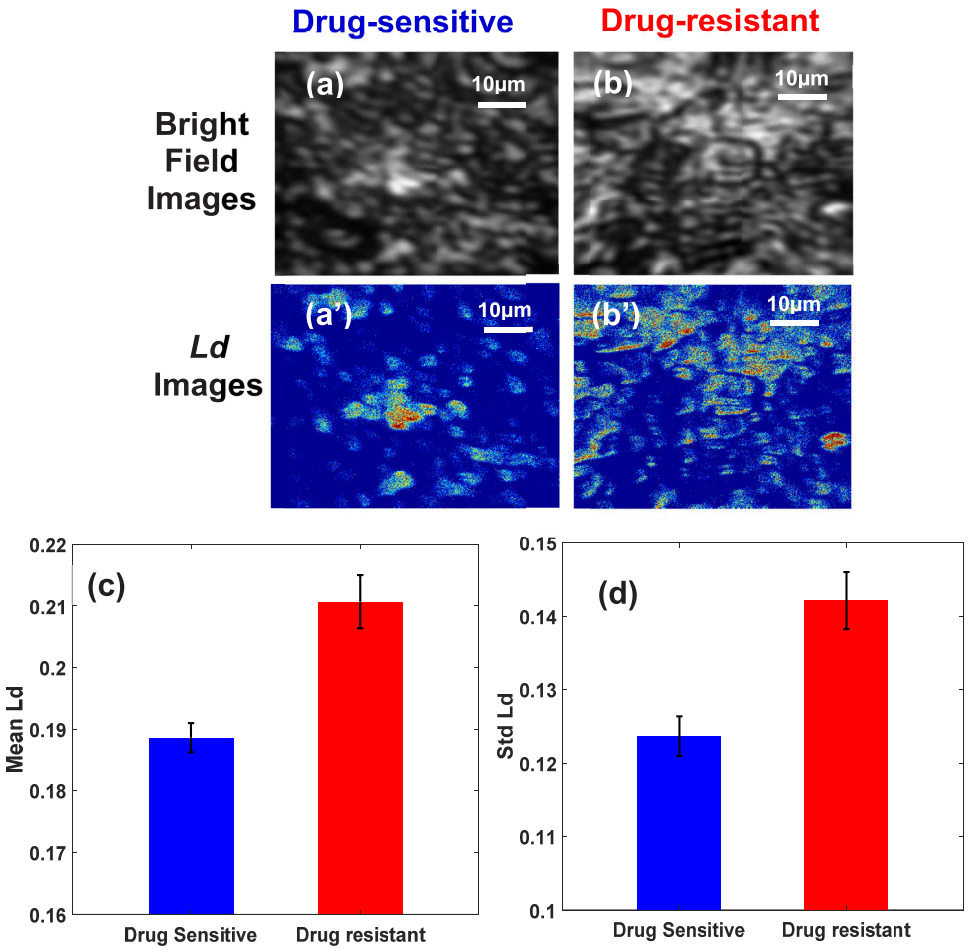

Fig. 3. (a) and (b) are the bright field images and (a') and (b') are the disorder strength, L_d images of tissues obtained by xenografting of drug-sensitive and drug-resistant PC cells line of PC3 type respectively. (c) and (d) are the bar graph representation of the mean and standard deviation of L_d of xenografted tumor respectively. Result shows 12% higher in the mean L_d and 15% increase in *std* L_d in a tumor developed from drug-resistant PC PC3 type cells line than the drug-sensitive cells. P-value < 0.05.

Biomedical Optics EXPRESS

than DU145 PC cell line is in strong agreement with their original PC cell line disorder strength. This confirms that the degree of disorder strength L_d can be used as a marker to detect the cancer stages or drug effects using 3D cancer tissue structure, similar to that of a cell line that is easy to study.

4. Conclusions

The results indicate that tumor tissues grown by xenografting of PC cells resistant towards docetaxel have a higher disorder strength L_d than the same tissues from drug-sensitive PC cells. Since the disorder strength increases with the increase in the level of tumorigenicity, which implies chemotherapy resistant cells are more aggressive than drug-sensitive cancerous cells. Cells from the prostate or any other cancerous region that survived through drug exposure are more aggressive and develop with the cell line's hierarchy as: PC3 > DU145 [8]. As an application of the developed finer focusing PWS technique, we have studied the structural alteration in the xenografted tissue morphology that are grown in a 3D environment from single cells that mainly have 2D structures. The results show metastasize isolated 2D cancer cells grown to 3D tumors in the body have similar structure and characteristics. The PWS analysis of 3D tissue slices confirms xenografted tissues from drug-resistant tumors have a higher average and standard deviation of disorder strength (L_d) than the drug-sensitive counterparts. Also, the obtained results follow a similar hierarchy of the cell lines that are studied earlier [8].

Probable cause of structural properties of drug resistance cells/tissues and higher structural disorder (L_d): Studies have shown that the progress of cancer disturbs the regular growth as well as the structure of cells/tissues. Further, cells/tissues that survive through the chemotherapy adapt themselves with the situation and develop different morphological structures resulting in higher mass density fluctuation due to the rearrangement of macromolecules, larger pore sizes, changes in cytoskeleton nanoarchitecture, etc. This results in a higher structural alteration in drug-resistant PC cells than drug-sensitive ones. The different mechanisms such as: tumor derived exosomes biogenesis and composition, DNA and histone damage/repair, anti-cancerous multidrug inactivation, alteration in drug targets treatment, heterogeneity in cancerous cells/tissues, death inhibition of cells/tissue, epithelial-mesenchymal transition and metastasis, etc. [27–31] are making the cancerous cells/tissues drug resistant [8]. Xenografted tumor tissues that are obtained using cells from drug-resistant and drug-sensitive PC cell lines, maintain the same types of structural hierarchy properties when they are grown into 3D structures. This supports a strong correlation in structural properties in 2D and 3D structures.

Applications of the developed technique for cancer treatment: The PWS study of xenografted tissues obtained from drug-sensitive and drug-resistant PC cells line could establish a new insight into advancing the understanding of the physical state and drug effectiveness on cancerous cells/tissues at the nanoscale level, by knowing their structural properties. The xenografted tissue structure replicating the structural properties of cancer cells explained statistically in term of the disorder strength L_d parameter could be a reliable, easy, and quantitative approach to diagnose chemo-resistance. This result seeks the potential application to monitor the effect of chemotherapy drugs on cancerous tissues and to study the different levels of tumorigenicity which can be obtained both, *in-vitro* and *in-vivo* methods. In summary, this method will help in understanding the drug-resistant and drug-sensitive cells/tissues and their different stages in the body, by examining their structural disorder properties.

Funding

National Institute of Health (K22 CA174994, R01 EB016983).

Biomedical Optics EXPRESS

Acknowledgements

National Institutes of Health (NIH) grants (No. R01EB016983) for Dr. Pradhan. Dr. Yallapu was supported by NIH K22 CA1748841.

Disclosures

The authors declare that there are no conflicts of interest in this article.

References

1. P. Pradhan, D. Damania, H. M. Joshi, V. Turzhitsky, H. Subramanian, H. K. Roy, A. Taflove, V. P. Dravid, and V. Backman, "Quantification of nanoscale density fluctuations using electron microscopy: Light-localization properties of biological cells," Appl. Phys. Lett. **97**(24), 243704 (2010).
2. P. Pradhan, D. Damania, H. M. Joshi, V. Turzhitsky, H. Subramanian, H. K. Roy, A. Taflove, V. Dravid, and V. Backman, "Quantification of Nanoscale Density Fluctuations by Electron Microscopy: probing cellular alterations in early carcinogenesis," Phys. Biol. **8**(2), 026012 (2011).
3. P. Wang, R. K. Bista, W. E. Khalbuss, W. Qiu, S. Uttam, K. Staton, L. Zhang, T. A. Brentnall, R. E. Brand, and Y. Liu, "Nanoscale nuclear architecture for cancer diagnosis beyond pathology via spatial-domain low-coherence quantitative phase microscopy," J. Biomed. Opt. **15**(6), 066028 (2010).
4. J. A. Nickerson, "Nuclear dreams: The malignant alteration of nuclear architecture," J. Cell. Biochem. **70**(2), 172–180 (1998).
5. D. Zink, A. H. Fischer, and J. A. Nickerson, "Nuclear structure in cancer cells," Nat. Rev. Cancer **4**(9), 677–687 (2004).
6. B. R. Konety and R. H. Getzenberg, "Nuclear structural proteins as biomarkers of cancer," J. Cell. Biochem. **75**(S32), 183–191 (1999).
7. P. Adhikari, F. Alharthi, and P. Pradhan, "Partial Wave Spectroscopy Detection of Cancer Stages using Tissue Microarrays (TMA) Samples," in *Frontiers in Optics + Laser Science APS/DLS (2019)* (Optical Society of America, 2019), paper JW4A.89.
8. H. M. Almabadi, P. K. B. Nagesh, P. Sahay, S. Bhandari, E. C. Eckstein, M. Jaggi, S. C. Chauhan, M. M. Yallapu, and P. Pradhan, "Optical study of chemotherapy efficiency in cancer treatment via intracellular structural disorder analysis using partial wave spectroscopy," J. Biophotonics **11**(12), e201800056 (2018).
9. S. Bhandari, P. Shukla, H. Almabadi, P. Sahay, R. Rao, and P. Pradhan, "Optical study of stress hormone-induced nanoscale structural alteration in brain using partial wave spectroscopic (PWS) microscopy," J. Biophotonics **12**(6), e201800002 (2019).
10. H. Subramanian, P. Pradhan, Y. Liu, I. R. Capoglu, J. D. Rogers, H. K. Roy, R. E. Brand, and V. Backman, "Partial-wave microscopic spectroscopy detects subwavelength refractive index fluctuations: an application to cancer diagnosis," Opt. Lett. **34**(4), 518–520 (2009).
11. H. Subramanian, P. Pradhan, Y. Liu, I. R. Capoglu, X. Li, J. D. Rogers, A. Heifetz, D. Kunte, H. K. Roy, A. Taflove, and V. Backman, "Optical methodology for detecting histologically unapparent nanoscale consequences of genetic alterations in biological cells," Proc. Natl. Acad. Sci. U. S. A. **105**(51), 20118–20123 (2008).
12. H. Subramanian, H. K. Roy, P. Pradhan, M. J. Goldberg, J. Muldoon, R. E. Brand, C. Sturgis, T. Hensing, D. Ray, A. Bogojevic, J. Mohammed, J.-S. Chang, and V. Backman, "Nanoscale Cellular Changes in Field Carcinogenesis Detected by Partial Wave Spectroscopy," Cancer Res. **69**(13), 5357–5363 (2009).
13. D. Damania, H. Subramanian, A. K. Tiwari, Y. Stypula, D. Kunte, P. Pradhan, H. K. Roy, and V. Backman, "Role of cytoskeleton in controlling the disorder strength of cellular nanoscale architecture," Biophys. J. **99**(3), 989–996 (2010).
14. P. Sahay, H. M. Almabadi, H. M. Ghimire, O. Skalli, and P. Pradhan, ""Light localization properties of weakly disordered optical media using confocal microscopy: application to cancer detection," Opt. Express **25**(13), 15428–15440 (2017).
15. P. Sahay, A. Ganju, H. M. Almabadi, H. M. Ghimire, M. M. Yallapu, O. Skalli, M. Jaggi, S. C. Chauhan, and P. Pradhan, "Quantification of photonic localization properties of targeted nuclear mass density variations: Application in cancer-stage detection," J. Biophotonics **11**(5), e201700257 (2018).
16. T. Freeman, "Photonic technique eases cancer staging," https://physicsworld.com/a/photonic-technique-eases-cancer-staging/.
17. B. Nijboer, "How to Reduce Stress at the Nanoscale Level," https://www.advancedsciencenews.com/how-to-reduce-stress-at-the-nanoscale-level/.
18. J. S. de Bono, S. Oudard, M. Ozguroglu, S. Hansen, J.-P. Machiels, I. Kocak, G. Gravis, I. Bodrogi, M. J. Mackenzie, L. Shen, M. Roessner, S. Gupta, and A. O. Sartor, and TROPIC Investigators, "Prednisone plus cabazitaxel or mitoxantrone for metastatic castration-resistant prostate cancer progressing after docetaxel treatment: a randomised open-label trial," Lancet **376**(9747), 1147–1154 (2010).
19. I. F. Tannock, D. Osoba, M. R. Stockler, D. S. Ernst, A. J. Neville, M. J. Moore, G. R. Armitage, J. J. Wilson, P. M. Venner, C. M. Coppin, and K. C. Murphy, "Chemotherapy with mitoxantrone plus prednisone or prednisone alone for

Biomedical Optics EXPRESS

symptomatic hormone-resistant prostate cancer: a Canadian randomized trial with palliative end points," J. Clin. Oncol. **14**(6), 1756–1764 (1996).
20. A. Yagoda and D. Petrylak, "Cytotoxic chemotherapy for advanced hormone-resistant prostate cancer," Cancer **71**(S3), 1098–1109 (1993).
21. J.-P. Gillet, A. M. Calcagno, S. Varma, M. Marino, L. J. Green, M. I. Vora, C. Patel, J. N. Orina, T. A. Eliseeva, V. Singal, R. Padmanabhan, B. Davidson, R. Ganapathi, A. K. Sood, B. R. Rueda, S. V. Ambudkar, and M. M. Gottesman, "Redefining the relevance of established cancer cell lines to the study of mechanisms of clinical anti-cancer drug resistance," Proc. Natl. Acad. Sci. U. S. A. **108**(46), 18708–18713 (2011).
22. S. Sumanasuriya and J. D. Bono, "Treatment of Advanced Prostate Cancer—A Review of Current Therapies and Future Promise," Cold Spring Harbor Perspect. Med. **8**(6), a030635 (2018).
23. C. L. Morton and P. J. Houghton, "Establishment of human tumor xenografts in immunodeficient mice," Nat. Protoc. **2**(2), 247–250 (2007).
24. Y. Ma, Z. Lin, J. K. Fallon, Q. Zhao, D. Liu, Y. Wang, and F. Liu, "New mouse xenograft model modulated by tumor-associated fibroblasts for human multi-drug resistance in cancer," Oncol. Rep. **34**(5), 2699–2705 (2015).
25. W. M. van Weerden and J. C. Romijn, "Use of nude mouse xenograft models in prostate cancer research," Prostate **43**(4), 263–271 (2000).
26. B. N. P. Kumar, N. Puvvada, S. Rajput, S. Sarkar, S. K. Das, L. Emdad, D. Sarkar, P. Venkatesan, I. Pal, G. Dey, S. Konar, K. R. Brunt, R. R. Rao, A. Mazumdar, S. C. Kundu, A. Pathak, P. B. Fisher, and M. Mandal, "Sequential release of drugs from hollow manganese ferrite nanocarriers for breast cancer therapy," J. Mater. Chem. B **3**(1), 90–101 (2015).
27. G. Housman, S. Byler, S. Heerboth, K. Lapinska, M. Longacre, N. Snyder, and S. Sarkar, "Drug resistance in cancer: an overview," Cancers **6**(3), 1769–1792 (2014).
28. M. Michael and M. M. Doherty, "Tumoral Drug Metabolism: Overview and Its Implications for Cancer Therapy," J. Clin. Oncol. **23**(1), 205–229 (2005).
29. W. Zhang, Y. Meng, N. Liu, X.-F. Wen, and T. Yang, "Insights into Chemoresistance of Prostate Cancer," Int. J. Biol. Sci. **11**(10), 1160–1170 (2015).
30. A. Persidis, "Cancer multidrug resistance," Nat. Biotechnol. **17**(1), 94–95 (1999).
31. L. Mashouri, H. Yousefi, A. R. Aref, A. mohammad Ahadi, F. Molaei, and S. K. Alahari, "Exosomes: composition, biogenesis, and mechanisms in cancer metastasis and drug resistance," Mol. Cancer **18**(1), 75 (2019).